Published in final edited form as:
Int J Cancer. 2009 March 15; 124(6): 1483–1489. doi:10.1002/ijc.24094.

Spindle assembly checkpoint and p53 deficiencies cooperate for tumorigenesis in mice

Ya-Hui Chi[1], **Jerrold M. Ward**[2], **Lily I. Cheng**[2], **Junichiro Yasunaga**[1], and **Kuan-Teh Jeang**[1,*]

[1]Molecular Virology Section, Laboratory of Molecular Microbiology, National Institute of Allergy and Infectious Diseases, National Institutes of Health, Bethesda, MD 20892, USA

[2]Infectious Disease Pathogenesis Section, Comparative Medicine Branch, Division of Intramural Research, National Institute of Allergy and Infectious Diseases, National Institutes of Health, Bethesda, MD 20892, USA

Abstract

The spindle assembly checkpoint (SAC) guards against chromosomal mis-segregation during mitosis. To investigate the role of SAC in tumor development, mice heterozygously knocked-out for the mitotic arrest deficient (Mad) genes *Mad1* and/or *Mad2* were mated with $p53^{+/-}$ mice. Increased tumor frequencies were reproducibly observed in $Mad2^{+/-}p53^{+/-}$ (88.2%) and $Mad1^{+/-}Mad2^{+/-}p53^{+/-}$ (95.0%) mice compared to $p53^{+/-}$ (66.7%) mice. Moreover, 53% of $Mad2^{+/-}p53^{+/-}$ mice developed lymphomas compared to 11% of $p53^{+/-}$ mice. By examining chromosome content, increased loss in diploidy was seen in cells from $Mad2^{+/-}p53^{+/-}$ versus $p53^{+/-}$ mice, correlating loss of SAC function, in a $p53^{+/-}$ context, with increased aneuploidy and tumorigenesis. The findings here provide evidence for a cooperative role of *Mad1/Mad2* and *p53* genes in preventing tumor development.

Keywords

Mad1; Mad2; p53; spindle assembly checkpoint; tumorigenesis

INTRODUCTION

The development and growth of organisms require faithful partitioning of the mother genome to daughter progenies. Genome integrity and cellular proliferation are regulated by elaborate networks that include cell-cycle checkpoints, DNA repair and recombination factors, and apoptosis regulators.1,2 Aberrations in these regulations can alter the structural integrity of chromosomes and/or induce chromosome instability (CIN).3–5 CIN is frequently associated with cancerous and pre-cancerous tissues.6,7 Mechanistically, the acquisition of a CIN phenotype may result in numerous changes in gene copies leading to the occurrence of genetic permutations and combinations that confer proliferative and survival advantages to cells.4,8

The different events that cause chromosomal mis-segregation are not completely understood.9,10 CIN cells lose or gain chromosome(s) with high frequency, suggesting that these cells are defective in some of the processes that govern orderly partitioning of

*Corresponding author: Building 4, Room 306, 9000 Rockville Pike, Bethesda, MD 20892-0460. Ph: (301) 496-6680; Fax: (301) 480-3686; Email: kj7e@nih.gov.

Novelty and impact: This manuscript describes the cooperative tumorigenic effects of deficiencies in spindle assembly checkpoint and the p53 tumor suppressor

chromosomes.11 The spindle assembly checkpoint (SAC) is one cellular mechanism that monitors the accuracy of chromosome segregation.12 The SAC was first identified when *Saccharomyces cerevisiae* was screened for genes required for fidelity of chromosome transmission.13,14 Currently, the SAC encompasses several proteins that are located at kinetochores, including the mitotic arrest deficient (MAD) proteins (MAD1, MAD2 and MAD3), the budding uninhibited by benzimidazole (BUB) proteins (BUB1, BUB2 and BUB3/BUBR1), the monopolar spindle 1 protein (MPS1), the ROD-ZW10-Zwilch complex, and the microtubule motor centromere protein E (CENP-E).15

Experimental findings are consistent with defects in SAC enhancing tumorigenesis.16,17 For example, individuals who are mutated in both alleles of the BubR1 protein develop childhood cancers (e.g. rhabdomyosarcoma and leukemia);18,19 and, up to 40% of human lung cancer cells carry defects in mitotic checkpoint genes, including *Mad1* and *Mad2*.20,21 In experimental mouse models, homozygous loss of SAC proteins (e.g. $Mad1^{-/-}$, $Mad2^{-/-}$, $BubR1^{-/-}$ or $Bub3^{-/-}$) are embryonic lethal.22–26 However, mice deficient in SAC function by virtue of a heterozygous knock-out of a single *Mad1*, *Mad2*, *BubR1*, *Bub3* or *CENP-E* allele are developmentally viable but show mildly increased rates of tumor development. Hence, $Mad1^{+/-}$, $Mad2^{+/-}$ and $CENP\text{-}E^{+/-}$ mice all have higher cancer rates compared to *wt* littermates.23,25,27 On the other hand, mice heterozygous for *BubR1* ($BubR1^{+/-}$) or *Bub3* ($Bub3^{+/-}$) do not present with constitutively higher rates of cancers; but, they, when exposed to carcinogens, do develop more tumors than similarly exposed *wt* mice.22,28,29

The p53 protein contributes to a checkpoint pathway distinct from the SAC. *P53* serves a G1/S checkpoint that detects structural DNA damage and is involved in an ATM(ATR)/CHK2(CHK1)-p53/MDM2-p21 cascade. Missense mutations in *p53* are common and are found in approximately 50% of human cancers.30 Mice haploinsufficient for *p53* develop sarcomas and lymphomas early in life.31 To date, although a published report has suggested that the loss of Mad2 and p53 contributes to chromosomal mis-segregation in MEFs,32 there are no *in vivo* data that address directly whether simultaneous haploinsufficiency in SAC and p53 cooperates in tumorigenesis.

Here, we have generated mice with the following compound genotypes: $Mad1^{+/-}p53^{+/-}$, $Mad2^{+/-}p53^{+/-}$ or $Mad1^{+/-}Mad2^{+/-}p53^{+/-}$. We have analyzed these mice for tumor incidence and tumor burden (i.e. multiple tumor types per mouse). We found enhanced cancer rates and increased tumor burden in mice doubly affected in both SAC and p53 compared to those singly attenuated for p53.

Materials and methods

Animals and genotyping

The $Mad1^{+/-}$ mice were generated by gene targeting as described previously.23 The $Mad2^{+/-}$ mice were a generous gift from Dr. Robert Benezra, the Memorial Sloan-Kettering Cancer Center. 25$Mad1^{-/-}$ and $Mad2^{-/-}$ mice are embryonic lethal and can not be used for cancer studies. The *p53*-deficient mice were purchased from the Jackson lab (strain: B6.129S2-$Trp53^{tm1Tyj}$/J).31 The Mad1, Mad2 and p53 knockout mice were all generated in C57BL/6 × 129/sv backgrounds.23,25,31 Genotypes of the mice were determined by polymerase chain reactions (PCRs) using primers: *Mad1* (5’ -cggacgaggtatttgcacgtgcagctctattttagg-3’ and 5’-gcatgggtgagctcagtcacactgg-3’);23*Mad2* (wt: 5’ -acctacgtcgccagtttccg-3’, mutant: 5’-tccattgctcagcggtgctg-3’ and common: 5’-ggggttcgcttctctacttgg-3’); *p53* (wt: 5’- acagcgtggtggtaccttat-3’, mutant: 5’-ctatcaggacatagcgttgg-3’ and common: 5’-tatactcagagccggcct -3’).31

Analyses of pathologies

Mice were necropsied and examined by mouse pathologists. All of the internal organs (spleen, liver, pancreas, kidney, stomach, intestine, lung, heart, brain, lymph node, thyroid gland) were fixed, paraffin embedded, sectioned and stained with H&E for analyses. Tissues that were found to be grossly abnormal at time of necropsy were multiply sectioned and stained by H&E (hematoxylin and eosin) for microscopic histological analyses.

Preparation of prometaphase chromosome spread from mouse spleen

Animals were sacrificed and spleens were dissected. Splenic cells were collected by forcing the spleen through a sterile 70μm nylon cell strainer (BD, Sparks, MD). The homogenized cells were cultured at 37°C in RPMI1640 medium supplemented with 10% fetal bovine serum (FBS), 5μg/mL concanavalin A (Sigma-Aldrich, St Louis, MO), 10μg/mL lipopolysaccharide (Sigma-Aldrich, St Louis, MO), 2 mM L-glutamine and antibiotics. After 24 to 48 hours of incubation, 10^{-7}M of methotrexate was added. 17 hours later, methotrexate was removed by washing the cells twice with RPMI 1640 complete media. Cells were resuspended in RPMI 1640 complete media containing 25 μg/ml BrdU (5-bromo-2-deoxyuridine) and incubated for another 5.5 hours. During the last 30 minutes of incubation, 0.06μg/ml demecolcine (Sigma-Aldrich, St Louis, MO) was added in order to arrest the cells in prometaphase. Cells were then pelleted by centrifugation, resuspended in warm hypotonic solution containing 0.075M KCl and incubated at 37°C for 15 minutes. Following incubation, a few drops of freshly prepared fixative (methanol:acetic acid=3:1) were added. Cells were washed with fixative 3 times, and chromosome spreads were prepared by dropping the cells onto chilled glass slides.

Fluorescent in situ hybridization

Dual-color fluorescent *in situ* hybridization (FISH) was performed using FITC-labeled probe specific for chromosome 11 and Cy3-labeled probe for chromosome 5 (Cambio Ltd, Cambridge, UK) according to the manufacturer's protocol. Briefly, slides with chromosome spreads of mouse cells were dehydrated with 100% ethanol, treated with pepsin and then denatured with 70% formamide/0.6xSSC at 65°C for 1.5 minutes. After 24 hours of hybridization with chromosomal paint probes, the slides were washed with 50% formamide/1xSSC, 1xSSC and 4xSSC/0.05% Tween20 successively. Finally, slides were mounted onto coverslips with antifade reagent (Invitrogen, Carlsbad, CA).

Statistical analyses

Tumor incidences were compared by the Fisher's exact probability test using the website: http://home.clara.net/sisa/fisher.htm. The statistical analysis of tumor numbers, survival curves, and spleen weights were computed using the PRISM software (version 5.01).

Results

Cooperative tumorigenicity of Mad1, Mad2 and p53 defects in mice

The mitotic checkpoint proteins Mad1, Mad2 and the p53 tumor suppressor protein function through different mechanisms. To investigate their potentially cooperative effects, we bred $Mad1^{+/-}Mad2^{+/-}$ mice with $p53^{+/-}$ mice to generate $Mad1^{+/-}p53^{+/-}$, $Mad2^{+/-}p53^{+/-}$, and $Mad1^{+/-}Mad2^{+/-}p53^{+/-}$ mutant mice. Genotype frequencies from the breedings produced offsprings that matched closely the expected numbers (Table 1), and these genetically distinct mice were monitored for tumor development. Animals that developed intractable pathologies were culled and necropsied as specified by the study protocol; and all the mice in the study groups were sacrificed at 18 months of age for analyses. In human Li-Fraumeni syndrome, germ line mutation occurs mostly in a single allele of the *p53* gene.[33–36] Thus,

we focused on mice with the $p53^{+/-}$ background in order to evaluate the early contribution from the loss of one p53 allele to the development of tumors.

We compared the four mouse cohorts for tumors (Fig. 1*a*). The trends showed increased tumor incidence in $Mad1^{+/-}Mad2^{+/-}p53^{+/-}$ (95% tumors) > $Mad2^{+/-}p53^{+/-}$ (88.2% tumors) > $Mad1^{+/-}p53^{+/-}$ (76.0% tumors) > $p53^{+/-}$ (66.7% tumors); there was a highly statistically significant (p=0.024, Fisher's exact test) difference in tumor incidence between $Mad1^{+/-}Mad2^{+/-}p53^{+/-}$ and $p53^{+/-}$ mice. We next quantified the tumor burdens in the four groups. Table 2 summarizes the tumor spectrum and frequencies observed in $p53^{+/-}$, $Mad1^{+/-}p53^{+/-}$, $Mad2^{+/-}p53^{+/-}$ and $Mad1^{+/-}Mad2^{+/-}p53^{+/-}$ mice. An expected baseline rate of lymphomas and sarcomas was seen in the $p53^{+/-}$ animals;30 however, notably, $Mad2^{+/-}p53^{+/-}$ mice (53%, 9 out of 17) showed a statistically significant (p=0.0077) increase in lymphoma frequency compared to $p53^{+/-}$ mice (11%, 2 out of 18) (Fig. 1*a*). Lymphoma-free survival curves between the two groups were also highly distinct (Fig. 1*b*). Moreover, the incidence of epithelial cancers, which is usually rare in $p53^{+/-}$ mice (1 out of 18 in our study) with C57BL/6 × 129/sv background,37–39 was substantially increased in $Mad2^{+/-}p53^{+/-}$ (3 out of 17) and $Mad1^{+/-}Mad2^{+/-}p53^{+/-}$ (4 out of 20) mice (Table 2).

We also noted that a partial loss of SAC function in the context of $p53^{+/-}$ produced larger tumor burdens per mouse (Table 2). In our study, $p53^{+/-}$ mice were either tumor free or invariably developed only a single type of tumor per mouse. By contrast, the $SAC^{+/-}p53^{+/-}$ compound mice were prone to have multiply different tumors per animal. On average, the tumor burden per $p53^{+/-}$ mouse was 0.61±0.12, and this number increased by 44% to 0.88±0.13 (p=0.16) in $Mad1^{+/-}p53^{+/-}$ mice, and more than doubled in both $Mad2^{+/-}p53^{+/-}$ (1.33±0.23; p=0.0082) and $Mad1^{+/-}Mad2^{+/-}p53^{+/-}$ (1.40±0.18; p=0.0012) animals (Fig. 1*c*). Some histological examples of tumors from the indicated mice are shown in Fig. 1*d*. Taken together, these *in vivo* results demonstrated that the compound $SAC^{+/-}p53^{+/-}$ animals when compared to $p53^{+/-}$ counterparts showed increased frequency of tumor development as well as increased numbers of tumors per mouse.

Above, we observed increased tumor burden in $Mad1^{+/-}Mad2^{+/-}p53^{+/-}$, $Mad1^{+/-}p53^{+/-}$, and $Mad2^{+/-}p53^{+/-}$ mice compared to the $p53^{+/-}$ animals. To understand these differences better, we also checked the tumor spectra and tumor burden of $Mad1^{+/-}$, $Mad2^{+/-}$, and $Mad1^{+/-}Mad2^{+/-}$ mice engineered with the $p53^{+/+}$ background. These latter mice were monitored for 18 months prior to necropsy and histopathological analyses (Table 3). Similar to previous reports from us and others,23,25 heterozygosity in *Mad1* and/or *Mad2* did increase the incidence of overall tumors in $p53^{+/+}$ mice. On the other hand, the incidence of lymphomas in $Mad2^{+/-}p53^{+/+}$ mice was no different than in *wt* $p53^{+/+}$ mice (also discussed by Michel et al, ref. 25), (Table 3). Thus the distinctly elevated lymphoma frequency in $Mad2^{+/-}p53^{+/-}$ mice compared to $p53^{+/-}$ animals is likely potentiated when dual genotypic defects co-exist. Above, we also noted that the triply mutated $Mad1^{+/-}Mad2^{+/-}p53^{+/-}$ mice developed novel tumor types (mammary adenocarcinoma, uterus-carcinoma and squamous cell carcinoma) that were not seen in either $p53^{+/-}$, or $Mad1^{+/-}$, or $Mad2^{+/-}$, or $Mad1^{+/-}Mad2^{+/-}$ mice. Collectively, these findings are consistent with the notion of cooperativity between the SAC and the *p53* pathway in preventing tumor formation.

Enlarged spleens in $Mad2^{+/-}p53^{+/-}$ mice

The high incidence of lymphoma in $Mad2^{+/-}p53^{+/-}$ mice (Fig. 1*a*, *b*) was correlated with a high frequency of enlarged spleens in these animals (Fig. 2*a*, *b*). On histological examination, *wt* spleens were well structured for red and white pulp (Fig. 2*c*, panel 1), while the white and red pulps were poorly demarcated in the $Mad2^{+/-}p53^{+/-}$ lymphomatous spleens (Fig. 2*c*, panel 5). By comparison, the boundaries (marginal zones) that separated white from red pulp in $p53^{+/-}$ lymphomatous spleens were not markedly disrupted (Fig. 2*c*,

panel 3). To better understand the cause of splenomegaly, we performed immunohistochemistry on *Mad2*$^{+/-}$*p53*$^{+/-}$ spleens staining for T-cell marker, CD3, and B-cell marker, Pax5 (Fig. 2*d*). The results were highly positive for CD3, but not for Pax5 (Fig. 2*d*), consistent with the presentation of T-cell anaplastic lymphoblastic lymphoma in *Mad2*$^{+/-}$*p53*$^{+/-}$ animals.

Loss of diploidy in Mad2$^{+/-}$p53$^{+/-}$ mouse cells

To ask why T-lymphomas were more aggressive in *Mad2*$^{+/-}$*p53*$^{+/-}$ compared to *p53*$^{+/-}$ mice, we wondered if the former was more prone to aneuploidy than the latter. We examined the frequency of chromosome mis-segregations in cells cultured from *wt*, *p53*$^{+/-}$, and *Mad2*$^{+/-}$*p53*$^{+/-}$ spleens. Dual-color FISH was employed to monitor the diploidy of mouse chromosomes 5 and 11 in the cells (Fig. 3*a*). Using identical culturing conditions, we triggered the proliferation of *wt*, *p53*$^{+/-}$, and *Mad2*$^{+/-}$*p53*$^{+/-}$ cells from the splenic explants using concanavalin A and lipopolysaccharide. Spindle toxin demecolcine was then used to arrest the cells in prometaphase, and we scored the karyotype of one hundred cells per genotype (repeated in two independent mice). Overall, 100% of the *wt* cells were diploid for both chromosome 5 and chromosome 11 (Fig. 3*b*); in *p53*$^{+/-}$ cells, the frequency of diploidy was reduced to 96% for chromosome 5 (3% triploid, 1% tetraploid) and 93% for chromosome 11 (3% monosomy, 1% triploid and 3% tetraploid); and the diploidy rate in *Mad2*$^{+/-}$*p53*$^{+/-}$ was further decreased to 87% [4% triploid, 6% tetraploid and 3% multiploid (>4) for chromosome 5; 3% triploid, 7% tetraploid and 4% multiploid (>4) for chromosome 11]. These results support that a SAC deficit in a *p53*$^{+/-}$ background increases cellular aneuploidy which was correlated with *in vivo* tumorigenesis in mice.

Discussion

An accepted view in cancer biology is that tumorigenesis emerges after the accumulation of multiple genetic changes. The “multi-hit” notion of cancer suggests that loss of function of some tumor suppressor genes (such as p53, pRB and BRCAs) could be a first step in cancer development. How and what additional *in vivo* steps cooperate subsequent to a “first step” remain incompletely understood.

Aneuploidy is present in more than 70% of human malignancies. It has been debated whether aneuploidy is causal or consequential of tumorigenesis. Previously, we and others have reported that heterozygous knock out in mouse of a single allele for one of several SAC genes increased the rate of cellular aneuploidy.22–25,27,40 Here, we asked in the context of a *p53*$^{+/-}$ genotype whether an additional defect in SAC function would increase *in vivo* cancer development. We found that mice with compound (*SAC*$^{+/-}$ + *p53*$^{+/-}$) genotypes were indeed more frequently tumorigenic [with *Mad1*$^{+/-}$*Mad2*$^{+/-}$*p53*$^{+/-}$ > *Mad2*$^{+/-}$*p53*$^{+/-}$ > *Mad1*$^{+/-}$*p53*$^{+/-}$ > *p53*$^{+/-}$ (Fig. 1*a*)], and showed higher tumor burden per mouse (Fig. 1*c*, Table 2). To our knowledge, this is the first report that a simultaneous deficit in SAC and p53 cooperates to increase *in vivo* cancer rates.

Currently, two major checkpoints employed by the cell have been proposed to maintain chromosomal integrity. One is the SAC in M phase41 composed by a complex of proteins, including Mad1 and Mad2; and the other is the G1/S checkpoint anchored by p53.42 Genetically damaged cells that fail either of these two checkpoints are arrested from progressing to the next phase of the cell cycle and may be subjected to apoptosis. Thus SAC and p53 act in different portions of the cell cycle and in different ways to prevent genetic damage that could provide the initiating event for cellular transformation. What could result if a cell were simultaneously defective in p53 and SAC? Here we report that mice defective for both p53 and Mad1 and/or Mad2 function were increased in tumor incidence compared to those mice singly defective for p53 or Mad1/2. Thus, our *in vivo* results are in agreement

with a published report of enhanced chromosome mis-segregation in cultured cells triggered by the simultaneous deletion of Mad2 and p53.32

In our mice, haploinsufficiency in Mad2 function contributed more significantly to tumor manifestation than comparable haploinsufficiency in Mad1. Current thoughts are that Mad1 recruits Mad2 to the spindle-unattached kinetochore converting an inactive Mad2 to its checkpoint-active, Cdc20-APC/C-competent, form.43⁻45 In this regard, Mad1 acts as a regulator of Mad2-effector function. *In vivo*, the higher tumor burden in $Mad2^{+/-}p53^{+/-}$*vs*. $Mad1^{+/-}p53^{+/-}$ animals (Fig. 1*c*) suggests that partial loss of the downstream Mad2 effector function is more potent for tumorigenicity than a corresponding deficit in the upstream Mad1 regulator.46

Finally, it is worth noting the different tumor spectra in $Mad1^{+/-}p53^{+/-}$, $Mad2^{+/-}p53^{+/-}$, $Mad1^{+/-}Mad2^{+/-}p53^{+/-}$, and $p53^{+/-}$ mice (Table 2). Collectively, the results suggest that different tissues may respond differently to individual and/or combined loss of p53 and SAC function. Thus, an earlier study had shown that $Mad2^{+/-}p53^{+/+}$ mice developed only papillary lung adenocarcinoma.25 Here, our $Mad2^{+/-}p53^{+/-}$ animals did have a modest increase in lung adenocarcinomas, but had a more substantial increase in lymphomas (Table 2). Curiously, our $Mad1^{+/-}Mad2^{+/-}p53^{+/-}$ cohort had a lower lymphoma rate than the $Mad2^{+/-}p53^{+/-}$ counterparts (Table 2). It may be that the mis-segregated chromosomes generated by a $Mad2^{+/-}p53^{+/-}$ genotype leads to carcinogenesis while further mis-segregations seen with the $Mad1^{+/-}Mad2^{+/-}p53^{+/-}$ geneotype create a substantially elevated genetic disorder which may trigger in certain lymphoid tissue cell death rather than cancer formation. Indeed, one such explanation was suggested for $CENP\text{-}E^{+/-}$ mice where a surfeit of aneuploidy actually decreased, not increased, tumor development.27 Thus, a possible take home lesson from the current study is that superimposed losses in checkpoint, rather than always being additive, could instead produce complex outcomes in the rates and types of tumors.

Abbreviations

Mad	mitotic arrest deficient
SAC	spindle assemble checkpoint
CIN	chromosome instability

Acknowledgments

We thank Dr. Robert Benezra of the Memorial Sloan-Kettering Cancer Center for providing $Mad2^{+/-}$ mice; Larry Faucette, Cindy Erexson, Elizabeth Williams and Dr. Torg Fredrickson in CMB, NIAID, NIH, for providing histopathological insights and excellent technical assistance; and members of the Jeang laboratory for critical readings of the manuscript. This work is supported by NIAID/NIH intramural funds and an NIAID contract to SoBran, Inc.

Reference List

1. Golias CH, Charalabopoulos A, Charalabopoulos K. Cell proliferation and cell cycle control: a mini review. Int J Clin Pract. 2004; 58:1134–1141. [PubMed: 15646411]
2. Massague J. G1 cell-cycle control and cancer. Nature. 2004; 432:298–306. [PubMed: 15549091]
3. Chi YH, Jeang KT. Aneuploidy and cancer. J Cell Biochem. 2007; 102:531–538. [PubMed: 17661351]
4. Gagos S, Irminger-Finger I. Chromosome instability in neoplasia: chaotic roots to continuous growth. Int J Biochem Cell Biol. 2005; 37:1014–1033. [PubMed: 15743675]

5. Rajagopalan H, Lengauer C. Aneuploidy and cancer. Nature. 2004; 432:338–341. [PubMed: 15549096]
6. Rajagopalan H, Nowak MA, Vogelstein B, Lengauer C. The significance of unstable chromosomes in colorectal cancer. Nat Rev Cancer. 2003; 3:695–701. [PubMed: 12951588]
7. Thurberg BL, Duray PH, Odze RD. Polypoid dysplasia in Barrett's esophagus: a clinicopathologic, immunohistochemical, and molecular study of five cases. Hum Pathol. 1999; 30:745–752. [PubMed: 10414492]
8. Weaver BA, Cleveland DW. Does aneuploidy cause cancer? Curr Opin Cell Biol. 2006; 18:658–667. [PubMed: 17046232]
9. Breivik J. The evolutionary origin of genetic instability in cancer development. Semin Cancer Biol. 2005; 15:51–60. [PubMed: 15613288]
10. Gollin SM. Mechanisms leading to chromosomal instability. Semin Cancer Biol. 2005; 15:33–42. [PubMed: 15613286]
11. Kops GJ, Weaver BA, Cleveland DW. On the road to cancer: aneuploidy and the mitotic checkpoint. Nat Rev Cancer. 2005; 5:773–785. [PubMed: 16195750]
12. Cleveland DW, Mao Y, Sullivan KF. Centromeres and kinetochores: from epigenetics to mitotic checkpoint signaling. Cell. 2003; 112:407–421. [PubMed: 12600307]
13. Kolodner RD, Putnam CD, Myung K. Maintenance of genome stability in Saccharomyces cerevisiae. Science. 2002; 297:552–557. [PubMed: 12142524]
14. Spencer F, Gerring SL, Connelly C, Hieter P. Mitotic chromosome transmission fidelity mutants in Saccharomyces cerevisiae. Genetics. 1990; 124:237–249. [PubMed: 2407610]
15. Yuen KW, Montpetit B, Hieter P. The kinetochore and cancer: what's the connection? Curr Opin Cell Biol. 2005; 17:576–582. [PubMed: 16233975]
16. Baker DJ, Chen J, van Deursen JM. The mitotic checkpoint in cancer and aging: what have mice taught us? Curr Opin Cell Biol. 2005; 17:583–589. [PubMed: 16226453]
17. Yuen KW, Montpetit B, Hieter P. The kinetochore and cancer: what's the connection? Curr Opin Cell Biol. 2005; 17:576–582. [PubMed: 16233975]
18. Hanks S, Coleman K, Reid S, Plaja A, Firth H, Fitzpatrick D, Kidd A, Mehes K, Nash R, Robin N, Shannon N, Tolmie J, et al. Constitutional aneuploidy and cancer predisposition caused by biallelic mutations in BUB1B. Nat Genet. 2004; 36:1159–1161. [PubMed: 15475955]
19. Matsuura S, Matsumoto Y, Morishima K, Izumi H, Matsumoto H, Ito E, Tsutsui K, Kobayashi J, Tauchi H, Kajiwara Y, Hama S, Kurisu K, et al. Monoallelic BUB1B mutations and defective mitotic-spindle checkpoint in seven families with premature chromatid separation (PCS) syndrome. Am J Med Genet A. 2006; 140:358–367. [PubMed: 16411201]
20. Coe BP, Lee EH, Chi B, Girard L, Minna JD, Gazdar AF, Lam S, MacAulay C, Lam WL. Gain of a region on 7p22.3, containing MAD1L1, is the most frequent event in small-cell lung cancer cell lines. Genes Chromosomes Cancer. 2006; 45:11–19. [PubMed: 16130125]
21. Takahashi T, Haruki N, Nomoto S, Masuda A, Saji S, Osada H, Takahashi T. Identification of frequent impairment of the mitotic checkpoint and molecular analysis of the mitotic checkpoint genes, hsMAD2 and p55CDC, in human lung cancers. Oncogene. 1999; 18:4295–4300. [PubMed: 10439037]
22. Dai W, Wang Q, Liu T, Swamy M, Fang Y, Xie S, Mahmood R, Yang YM, Xu M, Rao CV. Slippage of mitotic arrest and enhanced tumor development in mice with BubR1 haploinsufficiency. Cancer Res. 2004; 64:440–445. [PubMed: 14744753]
23. Iwanaga Y, Chi YH, Miyazato A, Sheleg S, Haller K, Peloponese JM Jr, Li Y, Ward JM, Benezra R, Jeang KT. Heterozygous deletion of mitotic arrest-deficient protein 1 (MAD1) increases the incidence of tumors in mice. Cancer Res. 2007; 67:160–166. [PubMed: 17210695]
24. Kalitsis P, Earle E, Fowler KJ, Choo KH. Bub3 gene disruption in mice reveals essential mitotic spindle checkpoint function during early embryogenesis. Genes Dev. 2000; 14:2277–2282. [PubMed: 10995385]
25. Michel LS, Liberal V, Chatterjee A, Kirchwegger R, Pasche B, Gerald W, Dobles M, Sorger PK, Murty VV, Benezra R. MAD2 haplo-insufficiency causes premature anaphase and chromosome instability in mammalian cells. Nature. 2001; 409:355–359. [PubMed: 11201745]

26. Wang Q, Liu T, Fang Y, Xie S, Huang X, Mahmood R, Ramaswamy G, Sakamoto KM, Darzynkiewicz Z, Xu M, Dai W. BUBR1 deficiency results in abnormal megakaryopoiesis. Blood. 2004; 103:1278–1285. [PubMed: 14576056]
27. Weaver BA, Silk AD, Montagna C, Verdier-Pinard P, Cleveland DW. Aneuploidy acts both oncogenically and as a tumor suppressor. Cancer Cell. 2007; 11:25–36. [PubMed: 17189716]
28. Babu JR, Jeganathan KB, Baker DJ, Wu X, Kang-Decker N, van Deursen JM. Rae1 is an essential mitotic checkpoint regulator that cooperates with Bub3 to prevent chromosome missegregation. J Cell Biol. 2003; 160:341–353. [PubMed: 12551952]
29. Kalitsis P, Fowler KJ, Griffiths B, Earle E, Chow CW, Jamsen K, Choo KH. Increased chromosome instability but not cancer predisposition in haploinsufficient Bub3 mice. Genes Chromosomes Cancer. 2005; 44:29–36. [PubMed: 15898111]
30. Soussi T, Lozano G. p53 mutation heterogeneity in cancer. Biochem Biophys Res Commun. 2005; 331:834–842. [PubMed: 15865939]
31. Jacks T, Remington L, Williams BO, Schmitt EM, Halachmi S, Bronson RT, Weinberg RA. Tumor spectrum analysis in p53-mutant mice. Curr Biol. 1994; 4:1–7. [PubMed: 7922305]
32. Burds AA, Lutum AS, Sorger PK. Generating chromosome instability through the simultaneous deletion of Mad2 and p53. Proc Natl Acad Sci U S A. 2005; 102:11296–11301. [PubMed: 16055552]
33. Metzger AK, Sheffield VC, Duyk G, Daneshvar L, Edwards MS, Cogen PH. Identification of a germ-line mutation in the p53 gene in a patient with an intracranial ependymoma. Proc Natl Acad Sci U S A. 1991; 88:7825–7829. [PubMed: 1679237]
34. Garber JE, Goldstein AM, Kantor AF, Dreyfus MG, Fraumeni JF Jr, Li FP. Follow-up study of twenty-four families with Li-Fraumeni syndrome. Cancer Res. 1991; 51:6094–6097. [PubMed: 1933872]
35. Volkers N. Of pedigrees, probes, and p53: 20 years of family studies. J Natl Cancer Inst. 1991; 83:1707–1709. [PubMed: 1770547]
36. Zambetti GP. The p53 mutation “gradient effect” and its clinical implications. J Cell Physiol. 2007; 213:370–373. [PubMed: 17671971]
37. Blackburn AC, McLary SC, Naeem R, Luszcz J, Stockton DW, Donehower LA, Mohammed M, Mailhes JB, Soferr T, Naber SP, Otis CN, Jerry DJ. Loss of heterozygosity occurs via mitotic recombination in Trp53+/−mice and associates with mammary tumor susceptibility of the BALB/c strain. Cancer Res. 2004; 64:5140–5147. [PubMed: 15289317]
38. Donehower LA, Harvey M, Vogel H, McArthur MJ, Montgomery CA Jr, Park SH, Thompson T, Ford RJ, Bradley A. Effects of genetic background on tumorigenesis in p53-deficient mice. Mol Carcinog. 1995; 14:16–22. [PubMed: 7546219]
39. Houghtaling S, Granville L, Akkari Y, Torimaru Y, Olson S, Finegold M, Grompe M. Heterozygosity for p53 (Trp53+/−) accelerates epithelial tumor formation in fanconi anemia complementation group D2 (Fancd2) knockout mice. Cancer Res. 2005; 65:85–91. [PubMed: 15665282]
40. Dobles M, Liberal V, Scott ML, Benezra R, Sorger PK. Chromosome missegregation and apoptosis in mice lacking the mitotic checkpoint protein Mad2. Cell. 2000; 101:635–645. [PubMed: 10892650]
41. Margolis RL, Lohez OD, Andreassen PR. G1 tetraploidy checkpoint and the suppression of tumorigenesis. J Cell Biochem. 2003; 88:673–683. [PubMed: 12577301]
42. Baek KH, Shin HJ, Yoo JK, Cho JH, Choi YH, Sung YC, McKeon F, Lee CW. p53 deficiency and defective mitotic checkpoint in proliferating T lymphocytes increase chromosomal instability through aberrant exit from mitotic arrest. J Leukoc Biol. 2003; 73:850–861. [PubMed: 12773518]
43. Chung E, Chen RH. Spindle checkpoint requires Mad1-bound and Mad1-free Mad2. Mol Biol Cell. 2002; 13:1501–1511. [PubMed: 12006648]
44. Kallio M, Weinstein J, Daum JR, Burke DJ, Gorbsky GJ. Mammalian p55CDC mediates association of the spindle checkpoint protein Mad2 with the cyclosome/anaphase-promoting complex, and is involved in regulating anaphase onset and late mitotic events. J Cell Biol. 1998; 141:1393–1406. [PubMed: 9628895]

45. Mapelli M, Massimiliano L, Santaguida S, Musacchio A. The Mad2 conformational dimer: structure and implications for the spindle assembly checkpoint. Cell. 2007; 131:730–743. [PubMed: 18022367]

46. Meraldi P, Draviam VM, Sorger PK. Timing and checkpoints in the regulation of mitotic progression. Dev Cell. 2004; 7:45–60. [PubMed: 15239953]

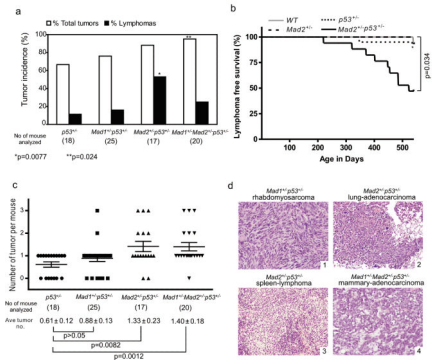

FIGURE 1.

A debilitated SAC elevated tumor formation in $p53^{+/-}$ mice. (*a*) Tumor incidences (by 18 months of age) in $p53^{+/-}$, $Mad1^{+/-}p53^{+/-}$, $Mad2^{+/-}p53^{+/-}$ and $Mad1^{+/-}Mad2^{+/-}p53^{+/-}$ mice. The number of mice in each group is denoted in brackets. Statistical significance ($p<0.05$, Fisher's exact test) between the indicated group and $p53^{+/-}$ littermates is denoted. (*b*) Lymphoma-free survival curves show an increased lymphoma incidence in $Mad2^{+/-}p53^{+/-}$ mice compare to $p53^{+/-}$, $Mad2^{+/-}$ or control wild type animals. Statistical significance ($p=0.034$) between $Mad2^{+/-}p53^{+/-}$ and $p53^{+/-}$ mutants was determined using log-rank test. (*c*) The number of tumor foci observed in $p53^{+/-}$, $Mad1^{+/-}p53^{+/-}$, $Mad2^{+/-}p53^{+/-}$ and $Mad1^{+/-}Mad2^{+/-}p53^{+/-}$ mice are shown. Mean ± s.d. for each cohort and *p*-values (t-test) between different groups are indicated. (*d*) Examples of tumor histology [hematoxylin and eosin (H&E)] from $Mad1^{+/-}p53^{+/-}$, $Mad2^{+/-}p53^{+/-}$ and $Mad1^{+/-}Mad2^{+/-}p53^{+/-}$ mice. Rhabdomyosarcoma from a 17 month old $Mad1^{+/-}p53^{+/-}$ mouse (panel 1), lung-adenocarcinoma from a 13 month old $Mad2^{+/-}p53^{+/-}$ mouse (panel 2), lymphoblastic lymphoma from a 12 month old $Mad2^{+/-}p53^{+/-}$ mouse (panel 3), and mammary adenocarcinoma from a 9 month old $Mad1^{+/-}Mad2^{+/-}p53^{+/-}$ mouse (panel 4) are shown.

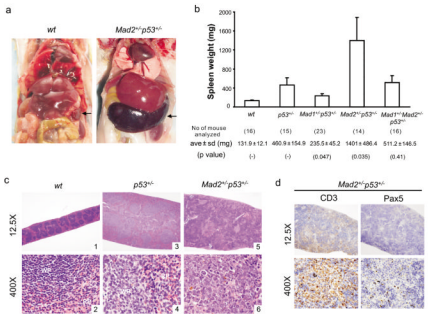

FIGURE 2.

Splenomegaly and increased lymphoma development in *Mad2*$^{+/-}$*p53*$^{+/-}$ mice. (*a*) A picture of an enlarged spleen in a *Mad2*$^{+/-}$*p53*$^{+/-}$ mouse (right). A wild type mouse (left) is shown for comparison. Spleens are indicated by arrows. (*b*) Mean mass and standard deviation of spleens freshly dissected from adult *wt*, *p53*$^{+/-}$, *Mad1*$^{+/-}$*p53*$^{+/-}$, *Mad2*$^{+/-}$*p53*$^{+/-}$ and *Mad1*$^{+/-}$*Mad2*$^{+/-}$*p53*$^{+/-}$ mice. *P*-values (t-test) between different groups and the *p53*$^{+/-}$ group are indicated in brackets. (*c*) H&E-stained sections of a *wt* normal spleen (panels 1–2) and lymphomatous spleens from *p53*$^{+/-}$ (panels 3–4) and *Mad2*$^{+/-}$*p53*$^{+/-}$ (panels 5–6) mice. Light microscopy images at low (12.5×) and high magnification (400×) are shown. WP, white pulp; RP, red pulp. (*d*) Immunohistochemistry of CD3 and Pax5 staining for a lymphomatous spleen from a *Mad2*$^{+/-}$*p53*$^{+/-}$ mouse. Hematoxylin was used to counterstain the nuclei. Images were taken at two magnifications (12.5× and 400×). The results show that the *Mad2*$^{+/-}$*p53*$^{+/-}$ spleens are grossly positive for T-cell marker CD3 but negative for B-cell marker Pax5.

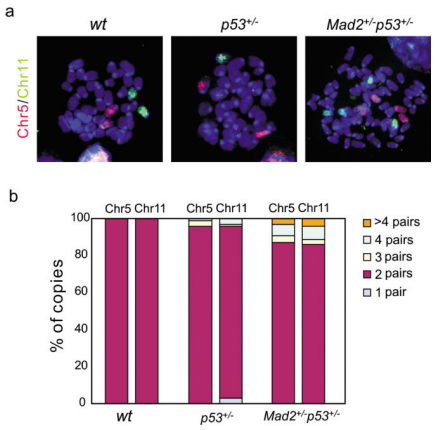

FIGURE 3.

Increased frequency of aneuploidy in *Mad2*$^{+/-}$*p53*$^{+/-}$ cells. (*a*) Detection of chromosome contents in *wt*, *p53*$^{+/-}$, and *Mad2*$^{+/-}$*p53*$^{+/-}$ cells by dual-color FISH using whole chromosome 11 (green) and chromosome 5 (red) specific probes. DNA was stained with DAPI (blue). (*b*) Histogram plot of chromosome counts (i.e. chromosome 11 and chromosome 5 stained by FISH) of cells from *wt*, *p53*$^{+/-}$ and *Mad2*$^{+/-}$*p53*$^{+/-}$ mice (two animals of each genotype were analyzed). One hundred metaphase spreads from each genotype were analyzed. The frequency of aneuploidy was significantly (p=0.0145, t-test, comparing *p53*$^{+/-}$ and *Mad2*$^{+/-}$*p53*$^{+/-}$) increased in *Mad2*$^{+/-}$*p53*$^{+/-}$ mice.

Table 1

Expected and actual genotype frequencies of the litters from parents that are heterozygous for *Mad1*, *Mad2* or *p53*. Representative litters from three breeder pairs are shown.

	breeder 1 (*wt* × *Mad1*$^{+/-}$*Mad2*$^{+/-}$*p53*$^{+/-}$)	breeder 2 (*Mad1*$^{+/-}$*Mad2*$^{+/-}$ × *p53*$^{+/-}$)	breeder 3 (*Mad1*$^{+/-}$*Mad2*$^{+/-}$ × *p53*$^{+/-}$)	Total	Expected frequency (%)	Actual frequency (%)
Mad1+/−Mad2+/−p53+/−	4	8	9	21	**12.5**	12.9
Mad1+/−p53+/−	7	4	12	23	**12.5**	14.1
Mad2+/−p53+/−	4	7	9	20	**12.5**	12.3
p53+/−	2	8	5	15	**12.5**	9.2
Mad1+/−Mad2+/−	1	12	8	21	**12.5**	12.9
Mad1+/−	4	10	7	21	**12.5**	12.9
Mad2+/−	3	8	10	21	**12.5**	12.9
wt	0	6	15	21	**12.5**	12.9
Total	25	63	75	163	100	100

Table 2

Tumor spectrum and burden in $p53^{+/-}$, $Mad1^{+/-}p53^{+/-}$, $Mad2^{+/-}p53^{+/-}$ and $Mad1^{+/-}Mad2^{+/-}p53^{+/-}$ compound mice.

Genotype # of mouse analyzed	$p53^{+/-}$ n=18	$Mad1^{+/-}p53^{+/-}$ n=25	$Mad2^{+/-}p53^{+/-}$ n=17	$Mad1^{+/-}Mad2^{+/-}p53^{+/-}$ n=20
lymphoma	2	4	9	5
osteosarcoma	3	7	4	9
giant-cell sarcoma	1	2	0	0
hemangiosarcoma	3	2	1	1
histocytic sarcoma	1	3	2	4
rhabdomyosarcoma	0	1	1	1
fibrosarcoma	0	0	1	1
skin-myxosarcoma	0	0	0	1
lung-adenocarcinoma	0	0	2	1
uterus-carcinoma	0	0	0	1
mammary adenocarcinoma	0	1	1	2
skin - squamous cell carcinoma	1	2	0	0
brain-medulloblastoma	1	0	0	0
# of tumors in mice	12	22	21	26
p value (compare to $p53^{+/-}$)	-	0.16	0.0082	0.0012

Table 3

Tumor spectrum in *wt*, *Mad1*$^{+/-}$, *Mad2*$^{+/-}$ and *Mad1*$^{+/-}$*Mad2*$^{+/-}$ with a *p53*$^{+/+}$ background.

Genotype **# of mouse analyzed**	***wt*** **n=23**	***Mad1*$^{+/-}$** **n=23**	***Mad2*$^{+/-}$** **n=22**	***Mad1*$^{+/-}$*Mad2*$^{+/-}$** **n=23**
lymphoma	1	2	1	3
lung-adenocarcinoma	2	2	2	2
liver-adenoma	0	1	1	0
histiocytic sarcoma	0	1	0	1
hemangiosarcoma	0	0	1	1
pituitary adenoma	0	1	1	1
osteosarcoma	0	0	1	1
# of tumors in mice	3	7	7	9